JEE Journal of Ecological Engineering

Journal of Ecological Engineering 2022, 23(5), 196–206
https://doi.org/10.12911/22998993/146783
ISSN 2299–8993, License CC-BY 4.0

Received: 2022.01.27
Accepted: 2022.03.14
Published: 2022.04.01

Solar Hot Water Heating and Electricity Generation Using PV/T Hybrid System

Ali A. Badran[1*], Firas A. Obeidat[1]

[1] Renewable Energy Engineering Department, Faculty of Engineering and Technology, Philadelphia University, Amman, Jordan

* Corresponding author's e-mail: abadran@philadelphia.edu.jo

ABSTRACT

Experimental work has been carried out to study the possibility of combining a conventional solar water collector with a hybrid device, developed previously and known as PV/T system, in order to obtain hot water with temperature above 40 °C. The effect of the combination on the productivity of hot water and the produced electricity was found. The formerly developed device, in which there was a multi-purpose solar collector, can produce hot water and electricity. It was connected to the conventional fin-tube collector in series in order to raise the product temperature to a higher level. This development was achieved for the first time as a combination between a PV/T and a conventional fin-tube collector. Instrumentation to measure temperatures, solar radiation, wind speed and flow rate was installed on the system. It was found that the water temperature was raised from 29 °C to 32 °C in the PV/T collector system and, after flowing through the conventional collector, it was raised to 50 °C and above. It was also found that the power efficiency in the case of water flow is always higher than in the case of no water flow.

Keywords: solar energy systems, water heating system, PV Module, flat-plate solar collector.

INTRODUCTION

Integrating a PV panel with a solar water heating system was first introduced by Wolf (1976]), and the concept of inverted water trickle used in the in a flat-plate collector was developed by Badran and Najjar (Badran Ali A et al, 1993). They built a new design of flat-plate collector that does not have finned tubes to conduct heat to water from the absorber plate. They named this system the inverted water trickle because heat was directly conducted to water from the absorber plate by means of a wire mesh that was fixed to the back of that plate. Later, Garg and Agrawal (1995) established a mathematical model for the PV/T collector system and solved it using the finite difference method. It was found that a normal domestic solar water heater of about 2 m^2 area generated sufficient electrical energy to run two tube lights of 20 W each for five hours and a TV set of 30 W capacity for 4 hours, in addition to heating 100 liters of water at 73 °C every hour.

At the local level, Al Mashaaleh (Al Mashaleh, Rebhi, 2012) built and tested a hybrid PV/T device in order to study its performance in the water heating mode. The inverted trickle flow regime was used here, where water was flowed on the backside of a PV solar panel using a jute layer to facilitate the water flow by gravity. Theoretical analysis was conducted in this study and it was compared with experimental results. It was found that the panel efficiency was increased by 28%, compared with a locally-made flat-plate collector, and the maximum overall efficiency of the hybrid PV/T system was 82%. The PV/T module produced 181.83 W of electric power in the presence of glass cover where the nominal electric power of the module was 250 Watts.

Badran and Al-Badadweh (2018) built and tested an improved hybrid inverted trickle PV/T solar system. The improvement was mainly the replacement of the jute layer at the back of the collector with a stainless-steel wire mesh layer. This replacement avoided the deterioration of the

jute layer over time which would occur otherwise and made it possible the use of material of high thermal conductivity, 17 W/mK for steel instead of 0.15 W/mK for jute.

Al-Bsoul and Badran (2016) built three modules of PV/T to investigate their performance under the same conditions. One module was using black monocrystalline cells sheet panel on black PV sheet, replacing the wooden frame with polyurethane foam and using a finned heat exchanger. The effects of those improvements were investigated theoretically and experimentally. It was found that using the black panel increased the thermal efficiency up to 4% and 20% with and without glazing, respectively, over that of the blue panel. In addition, using the polyurethane foam as a core structural material on the edges of the collector enhanced the thermal efficiency, and using the finned heat exchanger increased the productivity of desalinated water, reaching 3.33 l/m^2·day and 1.74 l/m^2·day with and without glazing, respectively. Moreover, it was found that glazing decreased electrical power output by 17.6%.

In order to investigate the effect of the feed flow rate on the performance of the system, two water flow rates at the input were used: 1.75 and 1 g/s. It was found that the highest electrical efficiency was 14.53%, which was obtained at 1.75 g/s. In this work, the adopted flow rate was 1.75 g/s.

THEORY

The difference between the conventional flat-plate collector and the PV/T trickle system is in the configuration, that is, the PV panel is used for generating electricity as well as being an absorber plate and that the trickled flow eliminates the need for using finned tubes.

The analyses of the conventional flat plate collectors are found in Duffie and Beckman (2013). The conventional flat plate analyses are applied on the PV/T trickle system, except for calculating the heat removal factor where the efficiency factor is one (Badran 1979). The performance of the PV/T system is based on performing energy balances on collector and desalination modes in order to find the instantaneous thermal, electrical and overall efficiencies, in addition to the productivity of the desalinated water. However, unfortunately, the device did not work properly in the desalination mode probably due to blockage of desalinated water outlet. Detailed treatment of the performance may be found in Badran and Badadweh (2018).

An energy balance on the PV/T collector reveals that:

$$\dot{E} = G\,P\,\eta_e\,[\,1 - \emptyset_c\,(T_c - 25)] \tag{1}$$

where: E – power used by the collector, W/m^2; G – solar irradiation, W/m^2; P – packing factor (A_{PV}/A_{system}) which is in this case equal to one; η_e – PV panel conversion efficiency; $\emptyset_c$ – solar cell temperature coefficient (1/°C).

The collector thermal efficiency of the PV/T trickle system is given by:

$$\eta_{th} = \frac{\mathrm{Q_u}}{A_c\,G} = F_R\,(\tau\alpha)_e - F_R\,U_L\,\frac{(T_\mathrm{i} - Ta)}{G} \tag{2}$$

where: η_{th} – thermal efficiency; F_R – collector heat removal factor; $(\tau\alpha)_e$ – effective transmittance-absorptance product; U_L – overall heat loss coefficient, W/m^2 °C; T_i – water input temperature °C. $F_R(\tau\alpha)_e$ – indicates how energy is absorbed, while F_RU_L – indicates how energy is lost.

In order to experimentally calculate thermal, electrical and overall efficiencies, the following equations are used:

$$\eta_{th} = \frac{\dot{\mathrm{m}}\,C_p\,(T_o - T_i)}{A_c\,G} \tag{3}$$

where: T_o – outlet water temperature, ºC

The electric efficiency of the PV panel is given by:

$$\eta_{el} = \frac{I\,V}{A_c\,G} \tag{4}$$

where: η_{el} – electrical efficiency; I – DC current from PV panel, amp.; V – DC voltage from the PV panel, V.

The overall efficiency is defined as the output divided by the input and is given by:

$$\eta_o = \frac{I\,V + \dot{\mathrm{m}}\,C_p\,(T_o - T_i)}{A_c\,G} \tag{5}$$

Hence:

$$\eta_o = \frac{I\,V}{A_c\,G} + \frac{\dot{m}\,C_p\,(T_o - T_i)}{A_c\,G} \qquad (6)$$

Equation 6 shows that the overall efficiency is obtained by the summation of electric and thermal efficiencies.

APPARATUS

The apparatus was set-up facing due South, as shown in Figure 1. The upper collector is the so-called inverted trickle solar collector. The frontal area of this collector is 1750×106 mm and the aperture area is 1630×950 mm. A cross section in this collector is shown in Figure 2.

The flow diagram of hot water is shown in Figure 3. The PV/T collector is on the top of the flat plate collector such that the flow will enter the PV/T first after being measured by the flow meter which is shown in Figure 9. The outlet of the PV/T is taken into the bottom of the flat-plate collector where the second stage of heating is supposed to take place. At the exit of the flat-plate collector at T_{02} is taken into the hot water storage tank. The temperature of water at the inlet of the first collector (T_1) is controlled by the hot water supply tank after which the water is taken to the flow meter and then to the PV/T inlet.

The lower collector was bought from the local market. It was made by a Spanish firm (delpaso. Solar), Model ECO 2000. The area of the lower collector is 2056×957 mm. Details of this collector are shown in Figure 4.

INSTRUMENTATION

The instrumentation is composed of several devices, the most important of which are; Pyranometer, which is a solar radiation meter device. The Integrator and Readout (Data Logger) is connected to the system do get the irradiance values and record them. The Pyranometer and the Integrator are shown in Figures 5 and 6.

Figure 1. General assembly for the apparatus

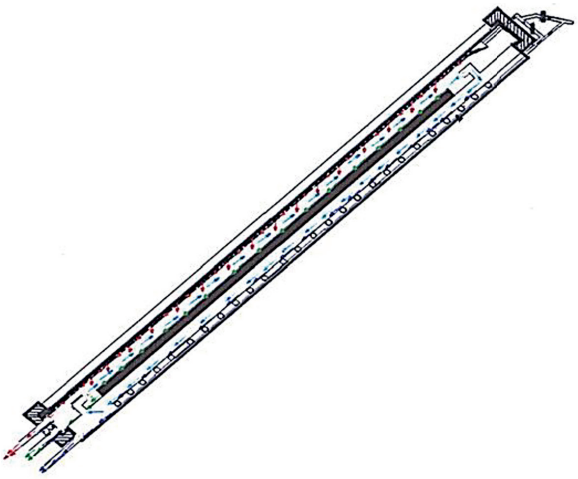

Figure 2. Inverted trickle PV/T collector

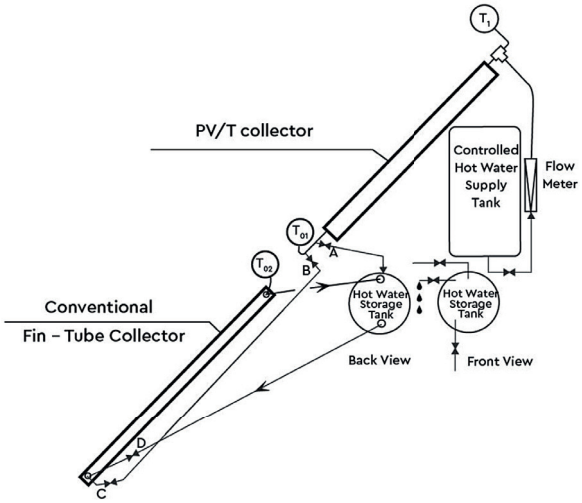

Figure 3. Flow diagram

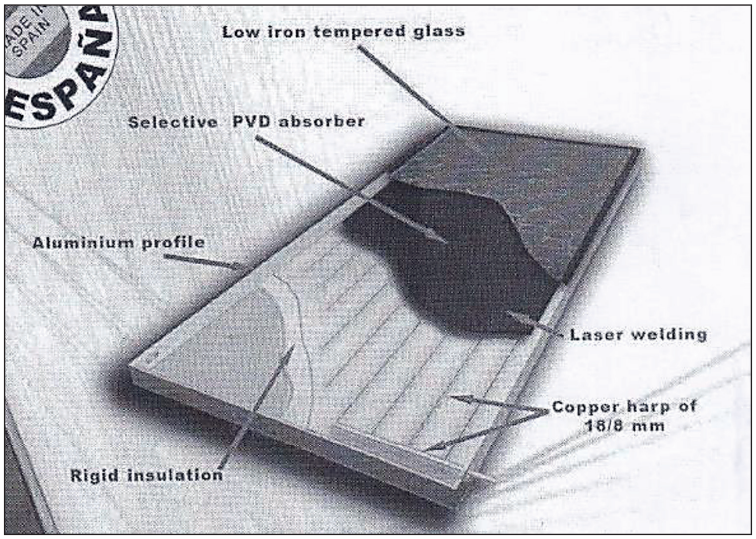

Figure 4. Fin-tube solar collector (Delpaso.solar)

Figure 5. Pyranometer

Figure 6. Solar integrator

Figure 7. Anemometer

Weather station

This is an automatic weather station that is composed of two parts: wind velocity meter and it is available at the University, see Figure 7, and a velocity reader type Young, see Figure 8. Both are available at the Wind Energy Lab.

Figure 8. Anemometer reader

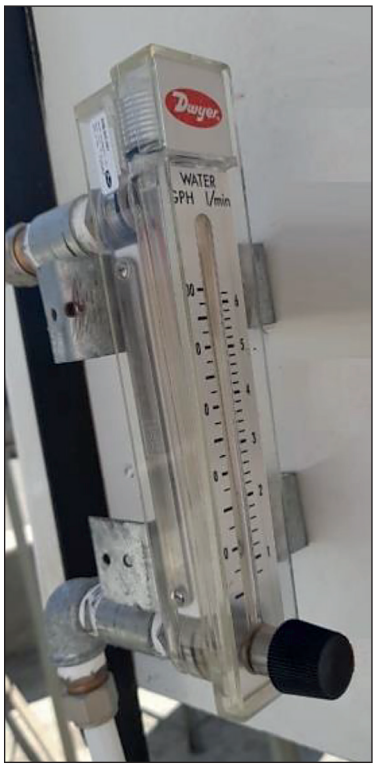

Figure 9. Flow meter

Flow meter

As shown in Figure 9, the flow meter (Dwyer Model RMB-SSV) is of 5-inch scale that is suitable for water. It is provided with a control valve for precision control.

Electric load

As shown in Figure 10, the electric load is composed of three resistances connected in parallel, 16 Ω, 100 W each, making a combined resistance equivalent of 5.3 Ω, and total rated power of 300 W. The resistances are housed in a plastic box provided with a fan for cooling.

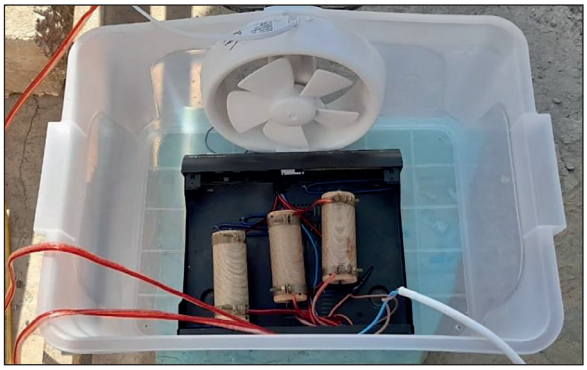

Figure 10. Electrical resistance load

Data acquisition system

The heart of the data acquisition system is the Arduino uno hardware, shown in Figure 11, The Arduino uno is used as a reader for the temperature and the current sensors. The Arduino uno sends the reading of the sensors every 10 minutes to a PC with a data logger software installed on it, the software data logger is called Teraterm. The temperature is measured using sensors with communication protocol called *one wire*, the sensors are from the type DS18b20 as shown in Figure 12. Moreover, the current is measured using the ACS712 20A module, as shown in Figure 13. This current sensor is read by the Arduino uno by the analog to digital conversion input port.

The voltage of the PV is measured by the Arduino uno with the help of a voltage divider, which reduces the voltage from the 18 V to 5 V

Figure 11. Arduino uno data logger

Figure 12. Temperature sensor DS18b20

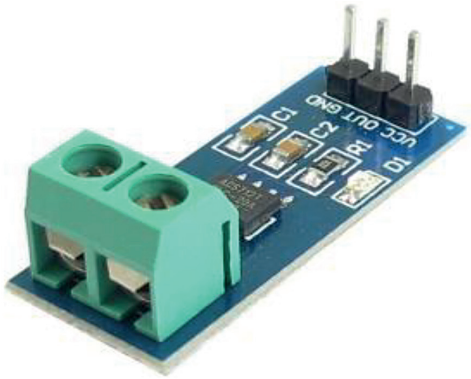

Figure 13. Current sensor ACS712 20A

scale to become compatible with the Arduino standard input levels.

EXPERIMENTAL DATA

This section contains the various parameters and specifications of the PV/T system, which are shown in Table 1 It also contains the actual data obtained of all experiments, which were conducted on the PV/T system during the period from 6–9 to 22-9-2021. Only the data obtained in 6-9-2021 and 22-9-2021 were retained, because they contain representative data for the whole testing period. Table 2 shows temperature legend for measuring points.

Table 2. Temperature legend

Symbol	Meaning
T_1	Water input temperature °C
T_{01}	Hybrid collector output temperature °C
T_{02}	Conventional collector output temperature °C
$T_{ambient}$	Ambient temperature °C

RESULTS AND DISCUSSION

It is noticed that irregularities in outlet temperature start to appear at mid-day (i.e.> 11:32 AM) and that is attributed to disturbance in flow. This disturbance is caused by air lock that the flow faces when it comes into contact with the liquid

Table 1. Parameters and specifications of the PV/T trickle system

Parameter		Symbol	Value	Unit
Latitude of position (Amman)		Φ	32N	Degrees
Longitude		L	36E	Degrees
Collector tilt angle		β	45°	Degrees
Collector azimuth angle		γ	0	Degrees
Average wind velocity		V	2	m/s
Collector (PV panel) area		A_C	1.64	m^2
Collector perimeter		perimeter	5.28	m
Collector thickness		L_C	0.10	m
Back insulation thickness		L_b	0.025	m
Edge insulation thickness		L_e	0.025	m
Absorptance of PV panel		α	0.903	Dimensionless
Emittance of PV panel		ε_p	0.80	Dimensionless
Thermal conductivity of the polyurethane		k_i	0.03	W/m.K
Water specific heat		C_p	4186	J/kg.ºC
Water inlet flow rate	Collector mode	$\dot{m}$	33.33	g/s
	Desalination mode	$\dot{m}$	1	
			1.75	
PV panel conversion efficiency		η	15.3	%
Solar cell temperature coefficient (1/ºC)		Φ	0.038	

in the lower collector. An attempt to avoid the occurrence of this phenomena was made but with minimum success, probably because the temperature at the outlet of the lower collector was too high, causing air to accumulate between the two collectors, which causes the blockage in the flow passage and therefore the disturbance in the flow. The flow of desalinated water was measured using a measuring cylinder between the PV/T and the conventional collector was 300 milliliters for the whole day. Therefore, combining the two systems in desalination mode was immaterial. Outlet water temperature, water input temperature, hybrid collector output temperature, conventional collector output temperature and ambient temperature are taken for the day 6/9/2021 as shown in Table 3 and all of these temperature degrees are drawn with time as shown in Figure 14.

One of the main purposes of this system is to generate the electricity, and as mentioned before, the system is connected to 300W resistive load to dissipate the generated power from the system. At each time, voltage, current, and power are recorded as shown in Table 4, and the power is drawn with time as shown in Figure 15.

Irradiance value for each time is recorded as shown in Table 5 using the pyranometer and the data logger which are connected between the system and a personal computer. These irradiance values are drawn with time as shown in Figure 16.

Only data in the afternoon of 22/9/2021 were retained because it contained representative data

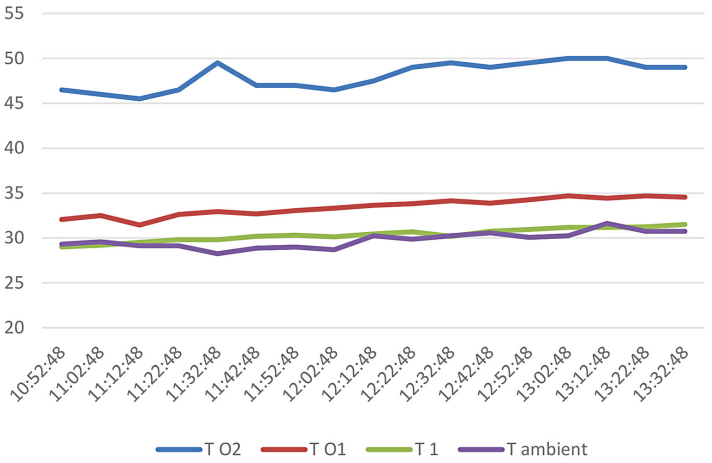

Figure 14. Temperature vs. time, 6/9/2021

Table 3. Variation of flow temperature from inlet to outlet of PV/T collector, 6/9/2021

Time	T_{02}	T_{01}	T_1	$T_{ambient}$	$T_{02} - T_1$	$T_{01} - T_1$
10:52:48 AM	46.5	32.06	29	29.31	17.5	3.06
11:02:48 AM	46	32.5	29.19	29.56	16.81	3.31
11:12:48 AM	45.5	31.44	29.5	29.12	16	1.94
11:22:48 AM	46.5	32.63	29.81	29.12	16.69	2.82
11:32:48 AM	49.5	32.94	29.81	28.25	19.69	3.13
11:42:48 AM	47	32.69	30.19	28.87	16.81	2.5
11:52:48 AM	47	33.06	30.31	29	16.69	2.75
12:02:48 PM	46.5	33.31	30.12	28.69	16.38	3.19
12:12:48 PM	47.5	33.63	30.44	30.25	17.06	3.19
12:22:48 PM	49	33.81	30.69	29.87	18.31	3.12
12:32:48 PM	49.5	34.13	30.19	30.25	19.31	3.94
12:42:48 PM	49	33.88	30.75	30.56	18.25	3.13
12:52:48 PM	49.5	34.25	30.94	30.06	18.56	3.31
1:02:48 PM	50	34.69	31.19	30.25	18.81	3.5
1:12:48 PM	50	34.44	31.19	31.62	18.81	3.25
1:22:48 PM	49	34.69	31.25	30.75	17.75	3.44
1:32:48 PM	49	34.56	31.5	30.75	17.5	3.06

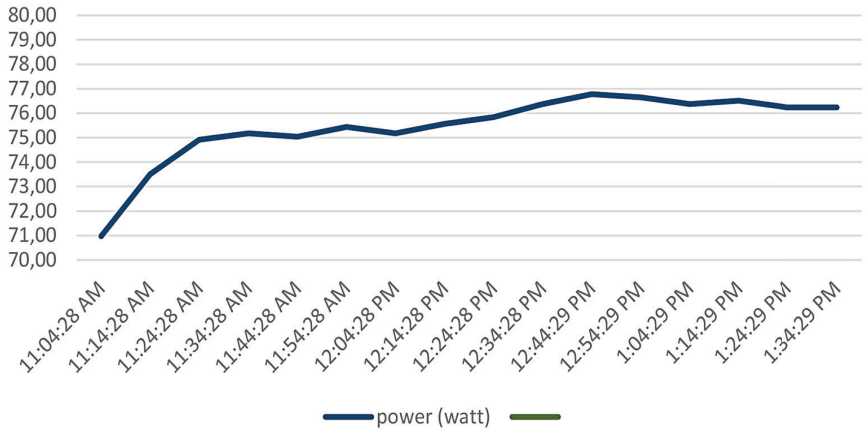

Figure 15. Power vs. time, 6/9/2021

Table 4. Power, 6/9/2021

Time	Voltage (V)	Current (A)	Power (Watt)
11:04:28 AM	17.49	4.06	70.97
11:14:28 AM	18.11	4.06	73.51
11:24:28 AM	18.46	4.06	74.91
11:34:28 AM	18.52	4.06	75.17
11:44:28 AM	18.49	4.06	75.04
11:54:28 AM	18.59	4.06	75.44
12:04:28 PM	18.52	4.06	75.17
12:14:28 PM	18.62	4.06	75.57
12:24:28 PM	18.68	4.06	75.83
12:34:28 PM	18.82	4.06	76.37
12:44:29 PM	18.92	4.06	76.78
12:54:29 PM	18.88	4.06	76.64
1:04:29 PM	18.82	4.06	76.37
1:14:29 PM	18.85	4.06	76.51
1:24:29 PM	18.78	4.06	76.24
1:34:29 PM	18.78	4.06	76.24

Table 5. Irradiance, W/m^2 ,6/9/2021

Time	Min.	Max.	Average
10:42:17 AM	773	804	788
10:52:17 AM	802	832	816
11:02:17 AM	831	865	847
11:12:17 AM	846	895	872
11:22:17 AM	886	913	900
11:32:17 AM	900	928	919
11:42:17 AM	925	948	937
11:52:17 AM	940	957	950
12:02:17 PM	953	961	957
12:12:17 PM	959	968	965
12:22:17 PM	961	974	966
12:32:17 PM	963	975	972
12:42:17 PM	966	977	973
12:52:17 PM	967	981	974
1:02:17 PM	966	974	970
1:12:17 PM	962	974	967
1:22:17 PM	962	967	965
1:32:17 PM	955	965	961

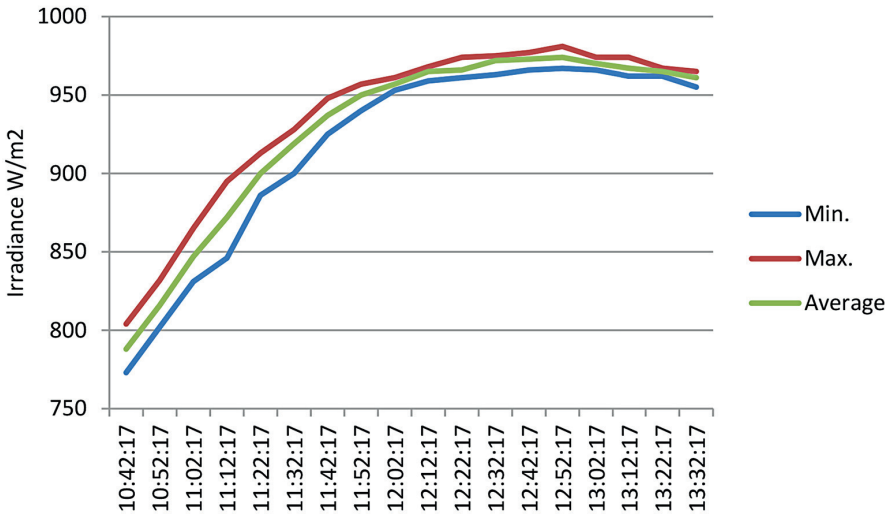

Figure 16. Irradiance vs time, 6/9/2021

Table 6. Irradiance, W/m^2, 22/9/2021

Time	Min.	Max.	Average W/m^2
12:17:52 PM	1017	1033	1025
12:27:52 PM	1025	1037	1031
12:37:52 PM	1027	1039	1033
12:47:52 PM	1030	1038	1035
12:57:52 PM	1021	1032	1025
1:07:52 PM	1013	1026	1018
1:17:52 PM	1013	1022	1018
1:27:52 PM	997	1020	1008
1:37:52 PM	989	1008	999
1:47:52 PM	976	997	984
1:57:52 PM	948	984	967

in the afternoon hours, which is shown in Table 6 and Figure 17 related to irradiance during the day of 22/9. The same is said about electric power during that day as shown in Table 7 and Figure 18.

The power efficiency curves show that the efficiency in the case of water flow is always higher than in the case without water flow as shown in Figure 19. In all previous readings, for example that of 9/6/2021, part of the readings were taken around the maximum value such that the reading is almost constant around that value.

For example, the average irradiance was calculated for that day as follows:

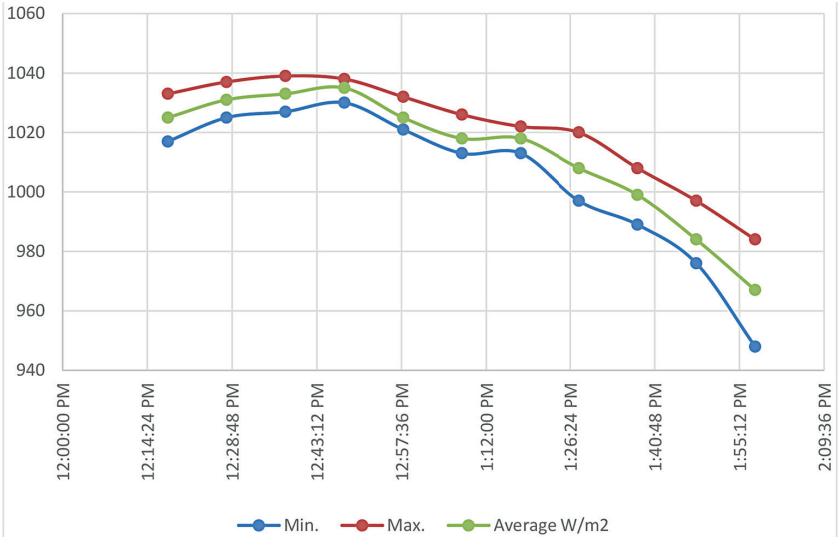

Figure 17. Irradiance vs. time, 22/9/2021

Table 7. Electric power, 22/9/2021

Time	Power W	Average Power W/m^2	Total power W	Efficiency 22/9	Efficiency 15/9	Efficiency increase
12:17:52 PM	68.4	1025	1678.95	4.1%	4.8%	18%
12:27:52 PM	69.6	1031	1688.778	4.1%	4.7%	14%
12:37:52 PM	69.9	1033	1692.054	4.1%	4.6%	12%
12:47:52 PM	72.8	1035	1695.33	4.3%	4.6%	6%
12:57:52 PM	72.8	1025	1678.95	4.3%	4.6%	5%
1:07:52 PM	72.0	1018	1667.484	4.3%	4.7%	9%
1:17:52 PM	71.9	1018	1667.484	4.3%	4.6%	6%
1:27:52 PM	71.5	1008	1651.104	4.3%	4.5%	5%
1:37:52 PM	72.6	999	1636.362	4.4%	4.5%	2%
1:47:52 PM	70.3	984	1611.792	4.4%	4.5%	4%
1:57:52 PM	71.1	967	1583.946	4.5%	4.7%	5%

Table 8. Efficiency of PV/T vs. ΔT/I

Parameters	6/9/2021	9/9/2021	12/9/2021	15/9/2021	8/9/2021
ΔT/I	0.0203	0.0235	0.0214	0.0215	0.022
η	0.173	0.107	0.193	0.109	0.16

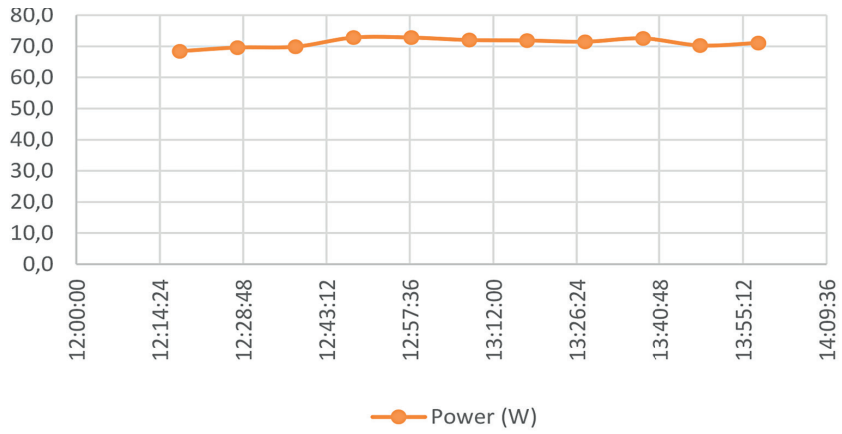

Figure 18. Power vs. time, 22/9/2021

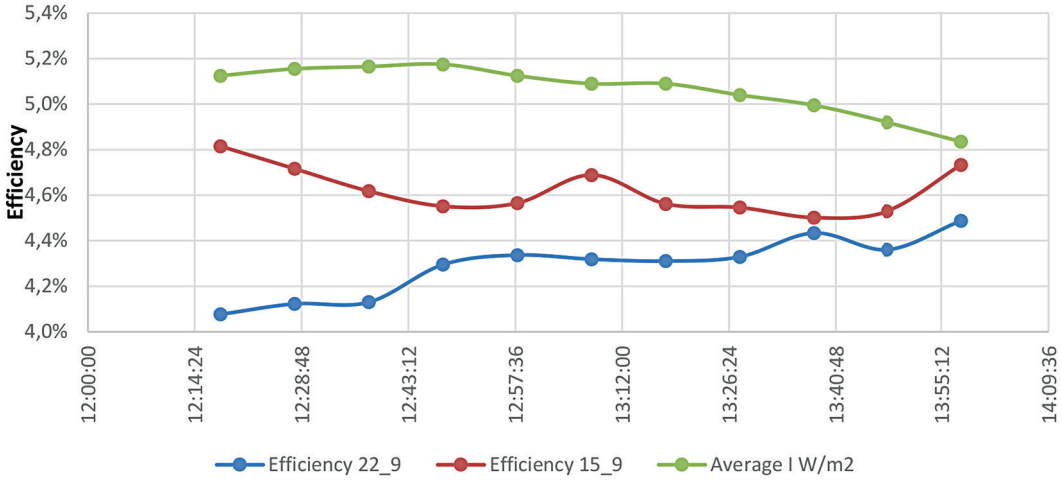

Figure 19. Efficiency comparison between PV/T with water flow in 15/9 and PV/T without water flow in 22/9

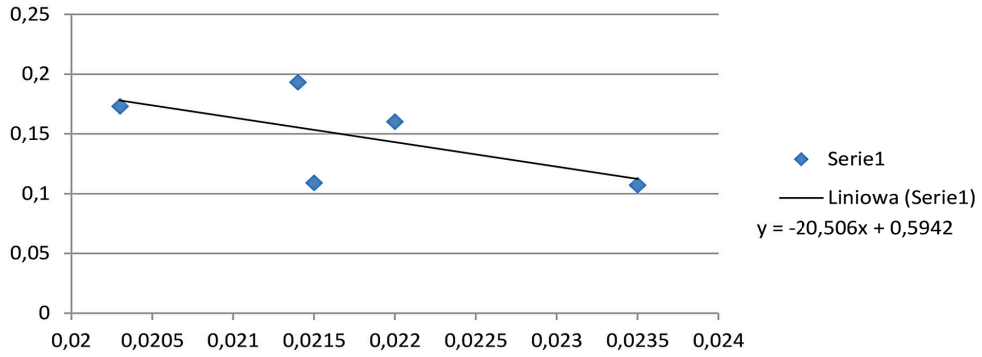

Figure 20. Instantaneous efficiency of PV/T vs. ΔT/I

$$I_{avg} = \frac{\sum I_{avg}}{i} = \frac{966 + 972 + 973 + 974 + 970 + 967 + 965}{7} = 969\ \mathrm{W/m^2} \quad (7)$$

And was taken as the maximum difference between T_{in} and T_{out} which occurred at 12:32 pm and equaled to 19.69 °C:

$$\frac{\Delta T_{max}}{I_{avg}} = \frac{19.69}{969} = 0.0209\ \mathrm{°C\ m^2/W} \quad (8)$$

Similarly, $\Delta T_{max}/I_{avg}$ can be found for the other dates and the efficiency can be found accordingly as shown in the Table 7.

The performance curve is shown in Figure 20 and the fitted line equation was found as: $y = -20.506x + 0.5942$, which is completely academic.

CONCLUSIONS

The aims of the project are achieved through showing the possibility of combining a conventional solar heater with a hybrid PV/T in series such that the water temperature achieved was above 40 °C. The effect of the above-mentioned combination on the productivity of hot water and the production of electricity from the hybrid device was found. However, the effect of this combination on desalinated water production is minimal and that was probably due to the fact that the flow rate was higher than necessary. It was noticed that irregularities in outlet temperature start to appear at some times; it was attributed to disturbance in flow. This disturbance is caused by air lock that the flow faces when it comes into contact with the liquid in the lower collector. The air lock is probably because of irregular supply from the upper collector and this irregular supply was found in the original water supply feeding the upper collector. The flow of desalinated water was measured using a measuring cylinder between the PV/T and the conventional collector was 300 milliliters for the whole day. Therefore, combining the two systems in desalination mode was immaterial. The means to avoid that air lock should be addressed.

Acknowledgements

The authors appreciate the support of deanship of research and graduate studies at Philadelphia University for the support of this work. The Authors also would like to appreciate the assistance of Eng. Ahmed Badran in carrying over this work.

REFERENCES

1. Wolf M. 1976. Performance analysis of combined heating and photovoltaic power systems for residences. Energy Conversion, 16(1–2), 79–90.
2. Badran A.A., Najjar Y.S.H. 1993. The inverted trickle flat plate solar collector. Int. J. Solar Energy, 14, 33–41.
3. Garg H., Agarwal K. 1995. Some aspects of a PV/T collector/forced circulation flat plate solar water heater with solar cells. Energy Conversion. Mgmt, 36(2), 87–99.
4. Al Mashaleh R. 2012. Theoretical analysis and experimental performance of a hybrid inverted trickle photovoltaic /thermal PV/T solar system. MSc. Thesis, Department of Mechanical Engineering, Faculty of Graduate Studies, University of Jordan.
5. Al Bsoul M. 2016. Performance of an improved hybrid inverted trickle photovoltaic/thermal (PV/T) solar system in the collector and desalination modes. MSc. Thesis, Department of Mechanical Engineering, Faculty of Graduate Studies, University of Jordan.
6. Badran A., Al Badadweh S. 2018. On the performanceof an improved hybrid inverted trickle photovoltaic / thermal (PV/T) solar system. 9th, Jordanian International Mechanical Engineering Conference (JIMEC 2018), Amman, Jordan 2018).
7. Duffie J., Beckman W. 2013. Solar Engineering of Thermal Processes, John Wiley and sons Inc., Fourth edition.